Adv Exp Med Biol - Advances in Microbiology, Infectious Diseases and Public Health (2020) 14: 1–19
https://doi.org/10.1007/5584_2019_431

Published online: 25 August 2019

Novel Polycationic Photosensitizers for Antibacterial Photodynamic Therapy

G. A. Meerovich, E. V. Akhlyustina, I. G. Tiganova, E. A. Lukyanets, E. A. Makarova, E. R. Tolordava, O. A. Yuzhakova, I. D. Romanishkin, N. I. Philipova, Yu. S. Zhizhimova, Yu. M. Romanova, V. B. Loschenov, and A. L. Gintsburg

Abstract

Antibacterial photodynamic therapy (APDT) is a promising method of treating local infected foci, in particular, surgical and burn wounds, trophic and diabetic ulcers. Photodynamic inactivation (PDI) is able to effectively destroy bacterial cells without them developing resistance in response to treatment.

This work was dedicated to the study of photophysical and antibacterial properties of new photosensitizers (PS) based on polycationic phthalocyanines and synthetic bacteriochlorins for photodynamic inactivation of *P. aeruginosa* bacteria and their biofilms. Gram-negative bacteria P. *aeruginosa* are often found in infected wounds, presumably in biofilm state and are characterized by rather low susceptibility to APDT, which is a problem. PS were studied for possible aggregation at various concentrations by means of absorption and fluorescence spectroscopy. The results of studies of the $ZnPcChol_8$, $(3\text{-}PyHp)_4BCBr_4$ and $(3\text{-}PyEBr)_4BCBr_4$ in water and serum confirm the assumption of a low degree of their aggregation at high concentrations.

G. A. Meerovich (✉) and V. B. Loschenov
Prokhorov General Physics Institute of the Russian Academy of Sciences, Moscow, Russia

National Research Nuclear University "MEPHI", Moscow, Russia
e-mail: meerovich@nsc.gpi.ru; gennadymeerovich@gmail.com; loschenov@mail.ru; loschenov@nsc.gpi.ru

E. V. Akhlyustina
National Research Nuclear University "MEPHI", Moscow, Russia
e-mail: katya_ahlyustina@mail.ru

I. G. Tiganova, E. R. Tolordava, N. I. Philipova, and Y. S. Zhizhimova
N.F. Gamaleya National Research Center of Epidemiology and Microbiology, Moscow, Russia
e-mail: iraida1tig@mail.ru; tolordavaeteri@mail.ru; merkyri_@mail.ru; zhizhimovaj@mail.ru

E. A. Lukyanets, E. A. Makarova, and O. A. Yuzhakova
Organic Intermediates and Dyes Institute, Moscow, Russia
e-mail: rmeluk@yandex.ru; ea_makarova22@yahoo.com; olganiopik@yandex.ru

I. D. Romanishkin
Prokhorov General Physics Institute of the Russian Academy of Sciences, Moscow, Russia
e-mail: igor.romanishkin@gmail.com

Y. M. Romanova and A. L. Gintsburg
N.F. Gamaleya National Research Center of Epidemiology and Microbiology, Moscow, Russia

I.M. Sechenov First Moscow State Medical University, Moscow, Russia
e-mail: genes2007@yandex.ru; Gintsburg@gamaleya.org

Consequently, their photodynamic efficiency is high enabling to use these PS at high concentrations to sensitize pathological foci for APDT.

It was shown that all the investigated PS had a high efficiency of photodynamic inactivation of Gram-negative bacteria *P. aeruginosa*, as well as their biofilms. Tetracationic hydrophilic near-infrared photosensitizer $(3\text{-PyEBr})_4\text{BCBr}_4$ with reduced molecule size had significantly higher efficacy of photodynamic inactivation of *P. aeruginosa* biofilms compared with other studied photosensitizers.

Keywords

Aggregation · Antibacterial photodynamic therapy; cationic photosensitizer · Bacterial biofilms · Bacteriochlorins · Luminescence

Abbreviations and Symbols

APDT	antibacterial photodynamic therapy
PDI	photodynamic inactivation
PS	photosensitizer
P. aeruginosa	Pseudomonas aeruginosa
S. aureus	Staphyllococcus aureus
A. baumannii	Acinetobacter baumannii
K. pneumoniae	Klebsiella pneumoniae
ZnPcChol_8	zinc octakis(cholinyl) phthalocyanine
$(3\text{-PyEBr})_4\text{BCBr}_4$	*meso*-tetrakis[1-(2′-bromoethyl)-3-pyridyl] bacteriochlorin tetrabromide
$(3\text{-PyHp})_4\text{BCBr}_4$	*meso*-tetrakis(1-heptyl-3-pyridyl)bacteriochlorin tetrabromide
Pc	phthalocyanine
Da	unified atomic mass unit or Dalton
CFU/ml	Colony Forming Units per milliliter
MBC	Minimal Bactericidal Concentration
Φ_F	quantum output of fluorescence
Φ_Δ	quantum yields of singlet oxygen
DNA	deoxyribonucleic acid
LB	Luria-Bertani medium

1 Introduction

Infected long-term non-healing complicated wounds of the skin and mucosa, trophic ulcers, pressure sores, ulcers of diabetic feet, represent serious problems for their treatment, especially in the case of resistant and multi-resistant pathogens. Approximately 1% of the population in both developed and developing countries faces these diseases (Bjarnsholt et al. 2011). In recent years, evidence has been obtained of the association of chronicity of wounds with biofilms, as well as with the presence of polymicrobial communities in the wound (Newton H et al. 2017). The exopolymer matrix of biofilms protects bacteria, in particular, from the effects of drugs and host immune defence factors, which complicates treatment. The main pathogens of wound infections are *Pseudomonas aeruginosa* (*P. aeruginosa*), *Staphyllococcus aureus* (*S. aureus*), *Acinetobacter baumannii*, *Klebsiella pneumoniae*, which can occur in the form of microbial associations. Antibiotic treatment in the case of a mature biofilm often gives only a temporary result, and even extensive debridement of the wound in combination with skin transplantation does not lead to rapid healing. Experts raise the question of the need for more effective methods of treating wounds (Bjarnsholt et al. 2011).

Antibacterial photodynamic therapy (APDT) is a promising way to treat infected surgical and burn wounds, trophic and diabetic ulcers (Park et al. 2011; Bertoloni et al. 1992; Percival et al. 2014) using light irradiation of lesions. The activation of photosensitizer (PS) by light, accompanied by the formation of singlet oxygen and other reactive oxygen species, leads to

multiple oxidative destruction of different subcellular structures of pathogens. Photodynamic process is able to effectively inactivate bacterial cells without developing resistance in response to the treatment, and, thanks to local irradiation, does not affect the normal microflora of the patient, as opposed to antibiotics (Nakonieczna et al. 2010; Tavares et al. 2010). The resistance to PS and APDT has not been detected even after 20 consequent cycles of the bacterial flora partial destruction followed by its regrowth (Hamblin and Hasan 2004; Vera et al. 2012). Almost all pathogenic microorganisms, including antibiotic-resistant strains of bacteria, are susceptible to APDT (Maisch 2015).

Chronic wound infections are often accompanied with biofilm formation, which are usually multi-species and include both Gram-positive and Gram-negative bacteria (Almeida et al. 2011). An effective PS must kill both Gram-positive and Gram-negative bacteria in planktonic as well as in biofilm state. Gram-positive and Gram-negative bacteria have fundamental differences in structure and charge of their cell wall, so they differ in sensitivity to drug effects. The sensitivity of Gram-negative bacteria to APDT is much lower compared to Gram-positive bacteria. The cell wall of Gram-positive bacteria has a relatively high degree of porosity. It is not a barrier for penetration by most PS, the molecular mass of which usually does not exceed 1500–1800 Da. The cell wall of Gram-negative bacteria prevents the penetration of large molecules and facilitates the resistance to many drugs (Nikaido 1994). Therefore, the inactivation of Gram-negative bacteria is the most important and difficult target for photodynamic treatment of infected foci (Maisch 2007).

Only polycationic PS with a rather small molecular mass effectively interact with Gram-negative bacteria. The efficiency of bacteria photodynamic inactivation depends on the properties of PS molecules – molecular mass (Meerovich et al. 2018), charge (number of cationic groups) (Simões et al 2016), photodynamic properties, in particular, the singlet oxygen quantum yield. The most likely mechanism ensuring the association of cationic PS with microbial cells is the electrostatic interaction of positively charged molecules with negatively charged sites of the cell walls.

Many studies of the photodynamic inactivation of Gram-negative bacteria were carried out using cationic phthalocyanines and bacteriochlorins

The cationic phthalocyanines are described in literature, carrying the positively charged substituents (Minnock et al. 1996; Griffith et al. 1997; Soncin et al. 2002; Vecchio et al. 2013; Roncucci et al. 2014; Ke et al. 2014; Spesia and Durantini 2013; Cakir et al. 2015; Colak et al. 2016; Zheng et al. 2013; Mantareva et al. 2013; Osifeko et al. 2015; Di Palma et al. 2015; Lourenço et al. 2015; Rocha et al. 2015; Segalla et al. 2002).

To ensure proper bacteria inactivation it is necessary to use high concentrations of PS during sensitization. The aggregation of tetrapyrrole molecules (van Lier and Spikes 1989; Moan 1984; Chowdhary et al. 2003) leads to a decrease in the intensity of absorption, the lifetime of the excited state of the PS, the quantum yield of fluorescence, as well as a change in the shape of the spectral absorption and fluorescence contours. The Coulomb repulsion of cationic PS molecules can partially diminish the aggregation. An increase in the number of substitutions (n) leads to a decrease of phthalocyanine aggregation degree in aqueous solutions and, consequently, to an increase of the quantum yield of fluorescence and singlet oxygen (Makarov et al. 2007, 2009; Strakhovskaya et al. 2009; Zhang et al. 2015). The rise of cationic phthalocyanines bactericidal photoactivity with n increase may be due both to the dissociation of inactive dimer complexes and increasing the efficiency of bacteria binding. As a result of our study it was found that octacationic zinc octakis(cholinyl)phthalocyanine $ZnPcChol_8$ has the highest bactericidal photoactivity (Kuznetsova et al. 2006; Yakubovskaya et al. 2015).

In bacterial biofilms, bacteria are additionally protected by a matrix, which significantly reduces the efficiency of photodynamic inactivation, primarily due to the fact that the matrix limits the diffusion of PS molecules and oxygen to bacteria.

The components of the matrix bind a significant part of photosensitizer molecules, including cationic ones, since the volume of the matrix is significantly larger than the total volume of bacteria. Therefore, a significant part of the light is absorbed by the sensitized matrix, consequently, a lot of photodynamic acts are realized at a distance from bacteria exceeding the free path of singlet oxygen (>1 μm), so it doesn't reach the bacterial cells.

It should be taken into account that the depth of the foci infected by *P. aeruginosa* can reach 12–15 mm (Bjarnsholt et al. 2011). Therefore, for the proper photodynamic effect on such foci, it is necessary to use PS, the excitation of which is carried out in the 720–850 nm spectral range – so called "biological tissue transparency window". Moreover, bacteria *P. aeruginosa* produce a number of pigments (in particular, pyocyanin, pyoverdin, pyorubrin, pyomelanin) in the course of their life in wounds (El-Fouly et al. 2015). The presence of these pigments in wound discharge leads to a large absorption in the 660–740 nm spectral range. Therefore, APDT with photosensitizers of the red spectral range may be ineffective due to the large losses of exciting light caused by absorption by both pigments and hemoglobin in host tissues. Thus, for the proper APDT of such foci, it is better to use the cationic PS excited in the 750–850 nm spectral range. That is why synthetic cationic derivatives of bacteriochlorins with intense absorption in near infrared spectral range of 760–850 nm are very promising as PS for APDT. Technological approaches proposed in (Mass and Lindsey 2011; Huang et al. 2010; Schastak et al. 2008, 2010; Dudkin et al. 2013a, b, 2014) allow the cationic derivatives of synthetic bacteriochlorins to be created with charges number from +4 to +8. The studies conducted on tetracationic and octacationic derivatives (Dudkin et al. 2013a, b) with a molecular weight of about 1500–1800 Da showed (Meerovich et al. 2016; Tiganova et al. 2017) that the PS can be used for the photodynamic inactivation (PDI) of Gram-positive bacteria *S. aureus* and Gram-negative bacteria *P. aeruginosa*. For these PS the values of their Minimal Bactericidal Concentration (MBC) were determined, which completely prevented the growth of bacteria.

This work was dedicated to the study of photophysical and antibacterial properties of new PS based on polycationic synthetic derivatives of phthalocyanines and bacteriochlorins designed for PDI of Gram-negative *P. aeruginosa* bacteria and their biofilms.

2 Materials and Methods

2.1 Synthesis of Photosensitizers

In our study, the original photosensitizers for photodynamic inactivation of bacteria and bacterial biofilms based on polycationic tetrapyrrole derivatives were synthesized in Organic Intermediates and Dyes Institute (Russia): zinc octakis(cholinyl)phthalocyanine $ZnPcChol_8$ with molecular mass 1678 Da, tetracationic bacteriochlorin derivatives: *meso*-tetrakis[1-(2′-bromoethyl)-3-pyridyl]-bacteriochlorin tetrabromide $(3\text{-PyEBr})_4BCBr_4$ with molecular mass 1374 Da and *meso*-tetrakis(1-heptyl-3-pyridyl)-bacteriochlorin tetrabromide $(3\text{-PyHp})_4BCBr_4$ with molecular mass 1339 Da (Fig. 1).

They showed high effectiveness in photodynamic inactivation of antibiotic resistant strains of Gram-negative bacteria (Vorozhtsov et al. 2006a, b; Meerovich et al. 2018).

The proposed method of synthesis of $ZnPcChol_8$ is presented in Fig. 2. The synthesis includes the chloromethylation of unsubstituted metal phthalocyanine and subsequent treatment of chloromethylated product with tertiary amines. In the case of diamines the resulting product was treated with methyl iodide doubling the number of cationic centres in the molecule.

The starting zinc phthalocyanine (ZnPc) was synthesized with yield of around 70% by heating the mixture of zinc acetate, *o*-phthalonitrile, N, N-dimethylaminoethanol and dimethylsulfoxide at 125–127 °C with subsequent dilution of chilled reaction mass by methanol, filtration of product and its multiple treatment with hot methanol

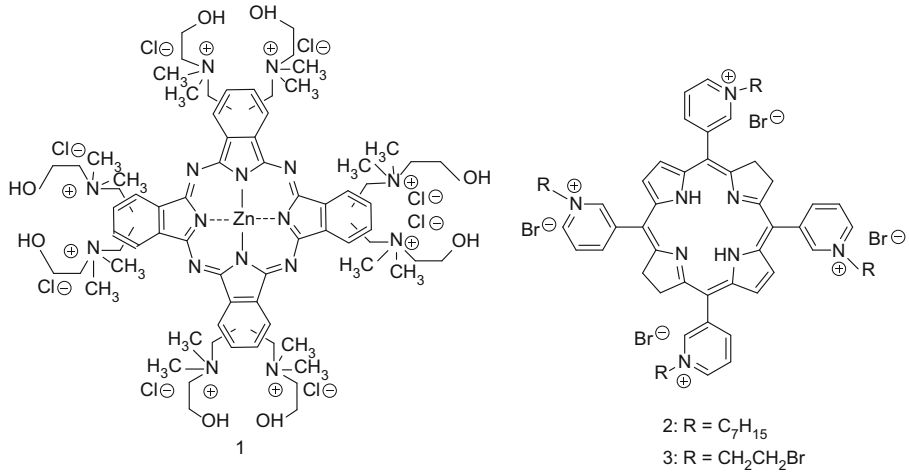

Fig. 1 The structures of the studied PS: 1 – $ZnPcChol_8$ (left); 2 – $(3\text{-}PyHp)_4BCBr_4$; 3 – $(3\text{-}PyEBr)_4BCBr_4$ (right)

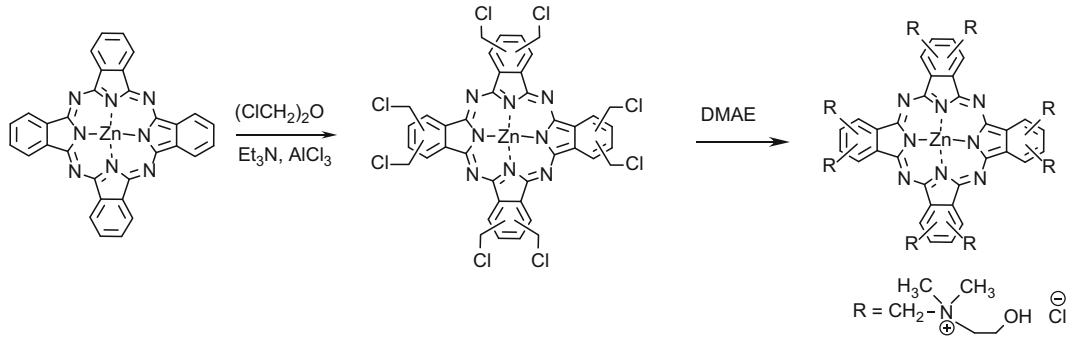

Fig. 2 The scheme of the synthesis of $ZnPcChol_8$

(Yuzhakova et al. 2005). We have developed the method of chloromethylation of ZnPc using a mixture of aluminum chloride, paraform and thionyl chloride at a temperature of 85–95 °C. This method allows high yield (above 90%) preparation of chloromethylated ZnPc with 7–8 substituents (Yuzhakova et al. 2010).

Tetracationic bacteriochlorin derivatives have been synthesized by alkylation of *meso*-tetra (3-pyridyl)bacteriochlorin with 1,2-dibromethane or heptyl bromide, respectively, in nitromethane in an inert atmosphere for 2 h (Makarova et al. 2018; Nevonen et al. 2018) (Fig. 3).

Compared to the tetracationic bacteriochlorins synthesized and studied by us earlier (Dudkin et al. 2014, Tiganova et al. 2017), the new PS have reduced molecular mass due to a decrease in the length of the alkylene chain from 4 to 2 methylene units in hydrophilic $(3\text{-}PyEBr)_4BCBr_4$ and from 11 to 7 carbon atoms in alkyl groups for amphiphilic $(3\text{-}PyHp)_4BCBr_4$.

2.2 Photophysical Studies of PS

The studies of the hydrophilic substances $ZnPcChol_8$ and $(3\text{-}PyEBr)_4BCBr_4$ were carried out in aqueous solutions, amphiphilic substance $(3\text{-}PyHp)_4BCBr_4$ was solubilized in 4% dispersion of Kolliphor ELP (BASF).

New PS were investigated *in vitro* for possible aggregation at various concentrations by means of absorption and fluorescence spectroscopy. The

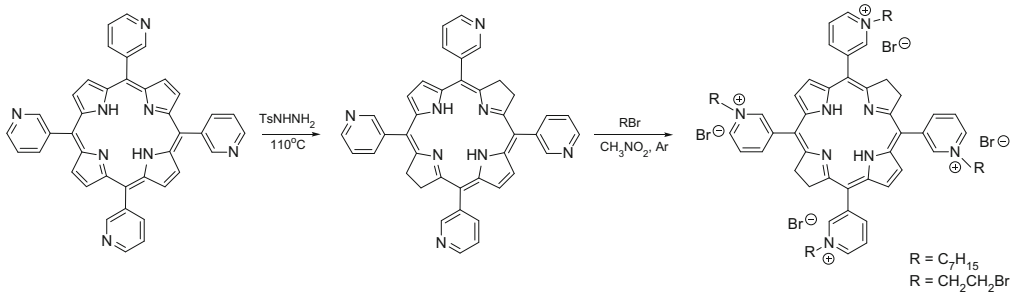

Fig. 3 The scheme of the synthesis of tetracationic bacteriochlorin derivatives

PS absorption in the concentration range from 0.001 mM to 0.1 mM was studied using a two-beam spectrophotometer "Hitachi U-3410" (Hitachi, Japan). Spectral-fluorescence studies were performed using a spectrum analyser "LESA-01-Biospec" (BIOSPEC, Russia). The fluorescence was excited by CW laser radiation at the wavelength of 532 nm (the second harmonic of the neodymium laser) coinciding with the Q_2-band of bacteriochlorin, and He-Ne laser with wavelength of 632.8 nm. To analyse the changes in the shape of the fluorescence spectral band of the PS, the measurements were performed in the cells of various lengths (1 mm and 10 mm). The shapes of the fluorescence spectral contours were calculated by dividing the intensity of the spectral signals by the intensity of their spectral maxima (so called "normalized fluorescence intensity").

For the evaluation of luminescence lifetime of PS the Hamamatsu streak-camera with a time-resolution was used. It comprised a laser source Picosecond Light Pulser "PLP-10" (Hamamatsu, Japan) with fibre optic output generating at the wavelength of 637 nm with a pulse duration of 65 ps and a polychromator with fibre optic input and Semrock optical filter "LD 01–785/10–12.5" or Omega Optical "660LP RapidEdge" inlet that transmits only the spectral region of luminescence band of bacteriochlorins or phthalocyanines (Bystrov et al. 2016). The image of the output slit of the polychromator was projected on the photocathode of the streak-camera, which included Streak scope "C10627–13" (Hamamatsu, Japan) with an adjustable time scan from 1 ns to 10 ms in the direction perpendicular to the image of the slit. The image from the output screen of Streak scope was received by the input of Digital CCD Camera "C9300–508". The synchronous delay generator "C10647–01" with a repetition rate of up to 1.6×10^7 Hz, synchronized the launch of the laser source and a Streak scope, allowing registering fluorescence signal with a spectral decomposition, and time base. The time-correlated counting method of single photons was used in the measurement process. The signal was recorded on a 5 ns time scan. The received signal was approximated by the function of two exponents with high accuracy of the approximation (5%).

2.3 Microbiological Studies

The microbiological studies were carried out on *P. aeruginosa* 32 and *P. aeruginosa* 21 clinical isolates. Bacteria were cultivated in LB-broth and 1% LB-agar (Difco, USA).

For the study of the photoinactivation of planktonic bacteria 18 h stationary phase broth culture was diluted 1:20 in LB broth and incubated 1.5 h at 37 °C with aeration. Bacterial suspension in saline was prepared with the initial content of bacteria 1×10^8 CFU/ml (Colony Forming Units per ml) by optical density. PS at different concentrations in water solutions were added in equal volumes to Eppendorf tubes with aliquots of bacterial suspension. After incubation with PS at 37 °C bacterial suspensions were centrifuged, supernatant was discarded and bacteria were resuspended in saline, aliquots of

100 μl from all samples and control (without PS) were placed in 96-well flat-bottom plates, one of them was irradiated, the other served as an unirradiated ("dark") control, every point in triplicate. The "SPD-M-685 LED" and "SPD-M-760 LED" light sources (BIOSPEC, Russia) at the wavelength of 685 and 760 nm were used for irradiation. "Coherent labmax" meter was used to control the power density. After irradiation, five 10-fold dilutions were prepared from every well and 20 μl from every dilution were plated on Petri dishes with LB agar. A day after, colonies were counted, amount of viable bacteria was estimated as CFU/ml, and means of 3 plates were plotted as a graph. It was estimated for standard conditions: incubation of bacteria with PS for 30 min, the dose of light 20 J/cm^2.

For estimation of bactericidal activity of PS on biofilms, the bacteria were grown for 20 h at 37 °C in 100 μl of LB in the wells of 96-well flat-bottom plates. Culture medium was replaced with water solution of PS at the desired concentration (every point in triplicate) and water for control and after 1 h incubation in the dark at 37 °C, PS was replaced with 100 μl of saline. Irradiation was performed with light dose 100 J/cm^2. To disaggregate biofilms, 11 μl of multienzyme substance ENZYMIX (BFR LABORATORIES, Russia) was added to every well for 10 min. The same procedures were performed for dark control plate. Five 10-fold dilutions were prepared from every well and 20 μl from every dilution were placed on Petri dishes. A day after, colonies were counted and the amount of viable bacteria was estimated as CFU/ml.

For spectral analysis of pigments production by biofilm, bacteria were grown in 20 ml of LB broth in Petri dishes for 1 or 3 days. Then the content of dishes was transferred into centrifuge tubes, vigorously vortexed and centrifuged at 7000 RPM for 15 min. Supernatant was filtered through 0,22 μ Millipore filter and vigorously shaked for good aeration before measurement.

Fluorescent microscopy technique was used for visualization of PDI results. The 18 h stationary broth culture was diluted 1:20 with fresh LB and added to glass cover slips. Young biofilms were formed in 3 h at 37 °C, then they were washed with distilled water and 50 μM of PS in water solution was added (the same volume of water was added for control). After 30 min of incubation in the dark, biofilms were washed 3 times with distilled water and irradiated with LED light sources mentioned above, except for the dark control. The glasses with biofilm were stained with Live/Dead Biofilm Viability Kit (Invitrogen Corp., USA) as specified, for 15 min. Pictures were taken and analyzed using fluorescent microscope Nikon H600L (Eclipse Ni) (Nikon Corp., Japan) using 20× objective, with subsequent overlay of images acquired with green and red filters.

3 Result and Discussion

3.1 Photophysical Studies

The absorption spectra of $ZnPcChol_8$, $(3\text{-}PyHp)_4BCBr_4$ and $(3\text{-}PyEBr)_4BCBr_4$ (Fig. 4) with a maximum wavelengths of about 677, 763 and 759 nm had a narrow band (34 nm for $ZnPcChol_8$, 28 nm for $(3\text{-}PyHp)_4BCBr_4$ and $(3\text{-}PyEBr)_4BCBr_4$).

The shape of the absorption spectra did not change with increasing concentration. The bathochromic shifted dimer band (Makarov et al. 2009) was absent in $ZnPcChol_8$ spectrum, as well as in $(3\text{-}PyEBr)_4BCBr_4$ and $(3\text{-}PyHp)_4BCBr$ spectra even at high concentrations. The absorption dependences on PS concentration was linear (Fig. 5). It agreed with extinction values determined at low concentrations. The experimental studies showed that the signs of aggregation in the absorption spectra behaviour of the studied octacationic phthalocyanine $ZnPcChol_8$ and tetracationic bacteriochlorin derivatives $(3\text{-}PyEBr)_4BCBr_4$ and $(3\text{-}PyHp)_4BCBr_4$ were not observed in the wide range of concentrations, up to 0.2 mM.

The results of PS absorption studying suggest that the degree of their aggregation at high concentrations was rather low.

As was shown in (Juzenas et al. 2004), the fluorescent properties of PS are more sensitive to aggregation than absorption properties. The fluorescence spectra of studied polycationic

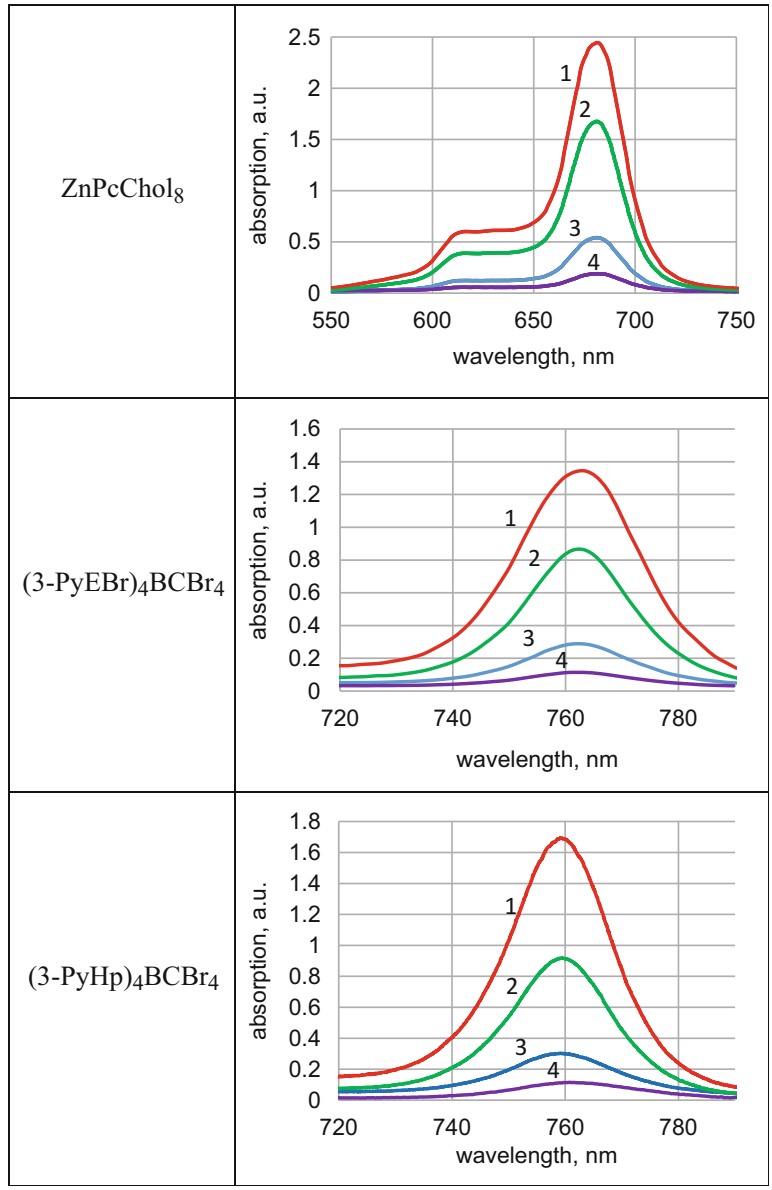

Fig. 4 The absorption spectra of $ZnPcChol_8$, $(3\text{-PyEBr})_4BCBr_4$ and $(3\text{-PyHp})_4BCBr_4$ at various concentrations: $ZnPcChol_8$: 1–0.15 mM; 2–0.1 mM; 3–0.03 mM; 4–0.01 mM. $(3\text{-PyEBr})_4BCBr_4$ and $(3\text{-PyHp})_4BCBr_4$: 1–0.2 mM; 2–0.1 mM; 3–0.03 mM; 4–0.01 mM

phthalocyanine and bacteriochlorin derivatives at concentrations of 0.005 mM are shown in Fig. 6.

The studied PS had a significant (>40%) overlap of the absorption and fluorescence spectral contours. Therefore, the process of reabsorption could affect their fluorescent properties at high concentrations (Fonin et al. 2014). So, fluorescent properties (the shape of the spectral contour of the fluorescence band, sublinear dependence of fluorescence intensity on concentration as well as value of the excited-state lifetime) at high concentrations could be caused by reabsorption, as well as aggregation (Dhami et al. 1995; Changenet-Barret et al. 2013). However, reabsorption, as a rule, did not affect the photodynamic efficiency, in contrast to aggregation, which reduces the effectiveness of PDT (Moan 1984). Therefore, it was important to assess which of the

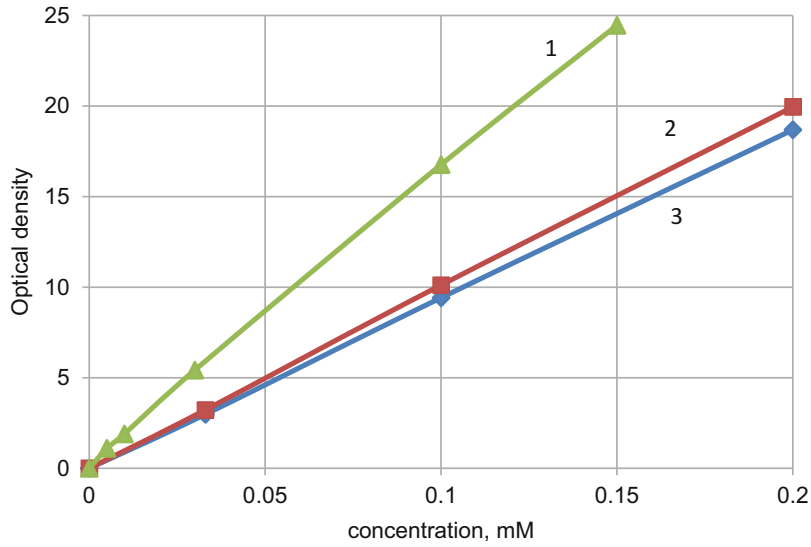

Fig. 5 The dependence of optical density of $ZnPcChol_8$ and $(3\text{-PyEBr})_4BCBr_4$ aqueous solutions (1,2), and $(3\text{-PyHp})_4BCBr_4$ in Kolliphor ELP nanodispersion (3), on their concentration

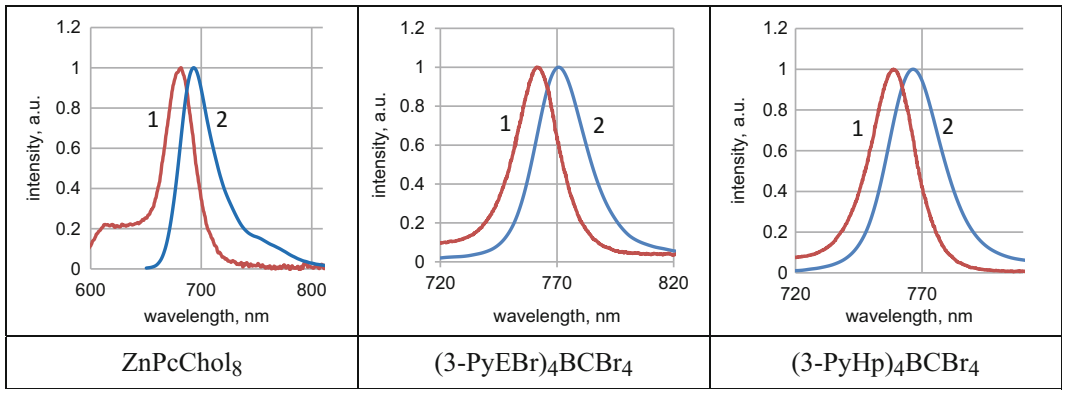

Fig. 6 The spectral contours of absorption (1) and fluorescence (2) bands of the studied PS at a low (0.005 mM) concentration

two phenomena dominates in the studied PS, especially at high concentrations. The signs of reabsorption in spectral-fluorescent studies, in contrast to the signs of aggregation, depended on the length of the cell (Juzenas et al. 2004). Therefore, spectral-fluorescent studies were carried out in cells 1 mm and 10 mm in length to separate the contributions of these phenomena and to evaluate the degree of aggregation of studied PS.

The shapes of the fluorescence spectra of $ZnPcChol_8$, $(3\text{-PyEBr})_4BCBr_4$ and $(3\text{-PyHp})_4BCBr_4$ at different concentrations in cells of various length are shown in Fig. 7.

Analysis of the spectra $ZnPcChol_8$ showed that an increase of cell length from 1 to 10 mm at low (0.005 mM) PS concentration does not affect the spectral shape (Fig. 8, A, spectra 1,2). This led only to a slight (1.8 nm) shift of the spectral maximum due to reabsorption, the fluorescence band remained narrow. At high concentrations (0.05 mM), a significant long-wavelength shift was observed, which depended on the length of the cell (5.8 nm – in a 1 mm long cell and 8.2 nm in a 10 mm cell). The shape of the spectra remained approximately the same. However, the half-width of the fluorescence

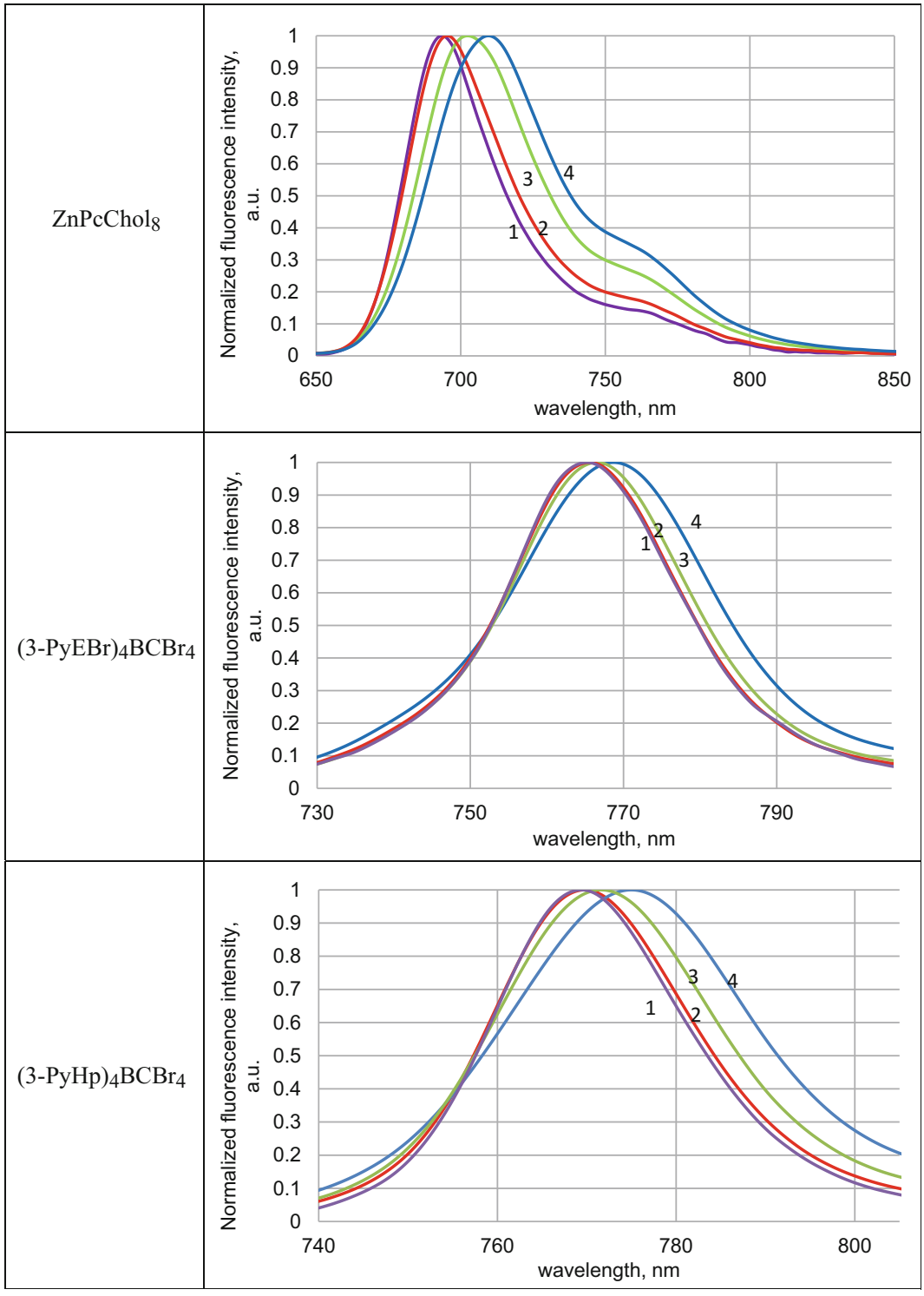

Fig. 7 The normalized fluorescence intensity (the shapes of the fluorescence spectra) of $ZnPcChol_8$, $(3\text{-PyEBr})_4BCBr_4$ and $(3\text{-PyHp})_4BCBr_4$ in cells of different lengths (1,3–1 mm; 2,4–10 mm) with concentrations: 1, 2–0.005 mM; 3,4–0.05 mM

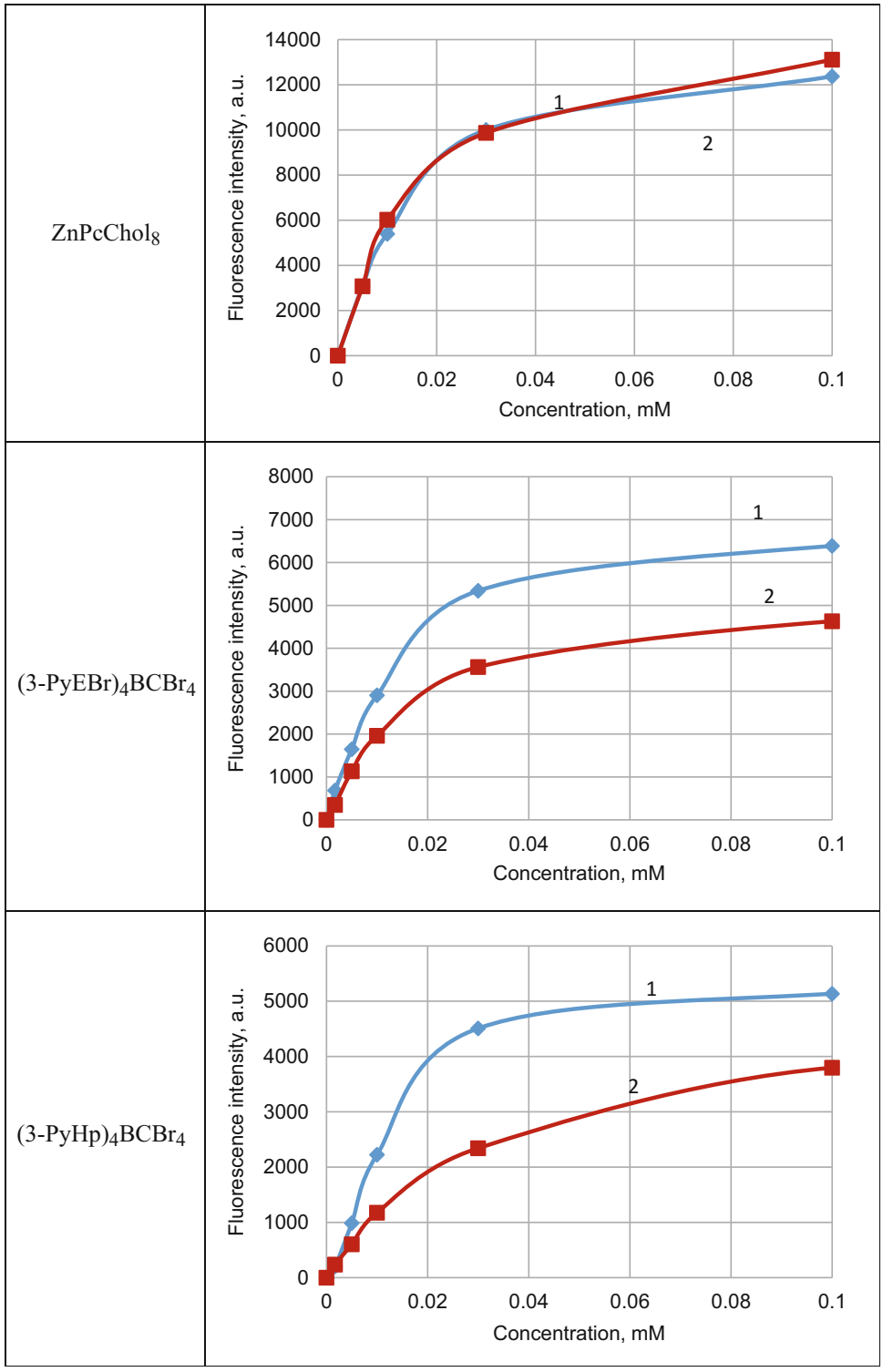

Fig. 8 The dependence of integral fluorescence intensity of $ZnPcChol_8$, $(3\text{-}PyEBr)_4BCBr_4$ and $(3\text{-}PyHp)_4BCBr_4$ on their concentration: (1) in water; (2) in serum

band increased: in the 1 mm cell – by 6.7 nm, and in the 10 mm cell – by 8.2 nm.

The analysis of the $(3\text{-PyEBr})_4BCBr_4$ and $(3\text{-PyHp})_4BCBr_4$ spectra showed that an increase of cell length from 1 to 10 mm at low (0.005 mM) PS concentration did not affect the spectral shape. This led only to a slight (0.3–0.4 nm) shift of the spectral maximum due to reabsorption, the fluorescence band remained narrow (27 nm). At high concentrations (0.05 mM, approximately corresponding to the PS concentration in blood 1 h after intravenous administration), a long-wavelength shift was observed, which depended on the length of the cell (at 2.2 nm – in a 1 mm long cell and at 5.6 nm in a 10 mm long cell). The shape of the spectra remained approximately the same. However, the half-width of the fluorescence band increased: in the 1 mm cell – by 3.3 nm, and in the 10 mm cell – by 6.9 nm.

This suggests that the observed phenomena at a high concentration are mainly associated with reabsorption and a weak aggregation (Dhami et al. 1995; Changenet-Barret et al. 2013; Juzenas et al. 2004).

The observed changes for $(3\text{-PyHp})_4BCBr_4$ were less than for $(3\text{-PyEBr})_4BCBr_4$. A long-wavelength shift of the spectral maximum of the fluorescence band occurs due to reabsorption at high concentrations (0.05 mM). The displacement depends on the length of cell (at 1.5 nm in a 1 mm cell and 3.4 nm in a 10 mm cell). The half-width of the fluorescence band in the 1 mm cell increased by 1.1 nm, and in the 10 mm cell – by 4.3 nm. The increase was much less than for $(3\text{-PyEBr})_4BCBr_4$. So, the observed changes occurring in $(3\text{-PyHp})_4BCBr_4$ at a high concentration are mainly associated with reabsorption; a weak aggregation takes place too but with a significantly smaller contribution (since the observed broadening is smaller).

It is known that aggregation of photosensitizers is lower in serum than in water (Tominaga et al. 1997). Therefore, some spectral fluorescence studies were carried out both in water and serum.

In the $ZnPcChol_8$ studies, the presence of two components in the solution was assumed: a monomeric PS with a lifetime in the range of 2.4–2.9 ns, and the second fluorescent component, possibly fluorescent dimer, with a significantly shorter lifetime (0.4–0.8 ns). In water, the share of the component with long lifetime, estimated by the number of photons with this lifetime among the total number of fluorescent photons, is about 94%. This allowed us to conclude that $ZnPcChol_8$ in the water does not aggregate in the studied range.

In the studies of $(3\text{-PyEBr})_4BCBr_4$ the presence of two components in the solution was also assumed: a monomeric PS with a lifetime in the range of 1.9–2.9 ns and its fluorescent dimer with a significantly shorter lifetime (<1 ns). In water, the share of the dominant component was about 74%. In serum, the lifetime was 2.4 ns; the share of the dominant component was higher (about 80–85% in the range below 0.1 mM). This correlated with the data (Tominaga et al. 1997) that in the blood plasma the aggregation of tetrapyrroles was lower in comparison with aggregation in water.

In the studies of the nanostructured $(3\text{-PyHp})_4BCBr_4$ fluorescence in water, the component with an average lifetime of 2.8 ns was dominant; its share was approximately 86%. In serum, the dominant component with an average lifetime of about 2.9 ns was almost 100%. This result was in good agreement with the data (Usacheva et al. 2001) that nanostructured PSs aggregate less in the aqueous environment at high concentrations.

Thus, the results of the fluorescence lifetime study also confirm that the aggregation of studied cationic PS at high concentrations (up to 0.1 mM) was low, especially in serum.

The results of integral fluorescence intensity study of $(3\text{-PyEBr})_4BCBr_4$ and $(3\text{-PyHp})_4BCBr_4$ depending on their concentration in water (1) and serum (2) are shown in Fig. 8.

The dependence of the fluorescence intensity of the $ZnPcChol_8$ on its concentration in water (1) was close to linear up to 0.03 mM; at higher concentration it became sublinear. The fluorescence intensity in serum was approximately the same as in water. The absence of aggregation in the selected concentration range was indirectly confirmed by the fact that, in studies in serum, there was practically no change in the shape of the fluorescence spectral band or an increase in its intensity.

The dependences of the integral fluorescence intensity of the $(3\text{-PyHp})_4BCBr_4$ nanodispersion as well as $(3\text{-PyEBr})_4BCBr_4$ solution on the concentration of PS were close to linear up to 0.03 mM in blood serum. At higher concentration they became sublinear. The same tendencies were observed for $(3\text{-PyHp})_4BCBr_4$ and $(3\text{-PyEBr})_4BCBr_4$ in water; their fluorescence intensity in water were lower in comparison with the fluorescence intensity in serum by approximately 1.3–1.4 and 1.5–2 times, respectively.

These results also suggest that in the most important for the APDT concentration range of <0.1 mM there were signs of both reabsorption and weak aggregation (aggregation is indicated by a lower fluorescence intensity in water compared to serum).

Thus, the results of spectral-fluorescence studies of the $(3\text{-PyHp})_4BCBr_4$ and $(3\text{-PyEBr})_4BCBr_4$ in water and serum confirmed the assumption of a low degree of their aggregation at high concentrations (Tominaga et al. 1997). Consequently, in the studied concentration range of these PSs, their photodynamic efficiency was high. This makes it possible to use these PS at high concentrations to sensitize pathological foci for APDT.

3.2 Light Absorption by Pigments in Non-sensitized P. aeruginosa Biofilm

P. aeruginosa bacteria produce pigments during biofilm growth, so culture medium becomes coloured. Analysis of spectral absorbance of culture medium of two clinical isolates revealed that the absorption of their pigments (presumably, pyocyanin) during the growth of a biofilm was practically negligible 5 h after the start of growth (data not shown). By hours 24 (by day 1), an intense band appeared in the absorption spectrum with a maximum at 690–700 nm, with a half-width of about 60 nm. The growth of this band continued for at least 3 days, its intensity depended on the strain of *P. aeruginosa*. The absorption spectra of pigments in the culture medium of two clinical isolates of *P. aeruginosa* 32 (A) and *P. aeruginosa* 21 (B) are shown in Fig. 9.

The optical density of pigments in culture medium of *P. aeruginosa 32* biofilms grown in LB broth reached high values at 690 nm (up to 1.8), which is close to the optical density of a variety of PS at effective concentration which are excited in this spectral region (in particular, $ZnPcChol_8$). It should be borne in mind that the concentration of pyocyanin in the spectrum of wound discharge during *P. aeruginosa* growth in the wound is much higher compared with biofilm growth in LB broth (El-Fouly et al. 2015).

4 Antibacterial Efficiency of the Studied Cationic PS

To assess the antibacterial efficiency of the studied cationic PS, viability of planktonic bacteria after photodynamic action was estimated under standard conditions (time of incubation of bacteria with PS was 30 min, light dose density of 20 J/cm^2). Dependence of viable bacteria amount on PS concentration is shown in Fig. 10. All photosensitisers tested had high efficiency against planktonic bacteria *P. aeruginosa* 32, which were completely inactivated after incubation with low concentrations of PS and irradiation: MBC of $(3\text{-PyEBr})_4BCBr_4$–2 μM, $(3\text{-PyHp})_4BCBr_4$–4 μM, $ZnPcChol_8$–5 μM). $(3\text{-PyEBr})_4BCBr_4$ had the lowest molecular weight (1374 Da), $ZnPcChol_8$ – the highest molecular weight among the studied PS (1678 Da). We suppose that smaller molecules have higher chance of penetration into the bacteria and this is a reason for the high efficacy of these PS. As was shown in (Usacheva et al. 2001), if PS is better at penetrating into the bacterial cell, the effectiveness of cell inactivation is higher. The high antibacterial efficacy of the studied PS is due to the fact that they are effectively associated with Gram-negative bacteria *P. aeruginosa* due to the large (4–8) number of cationic substituents and do not aggregate even at high concentrations.

These PS had significantly lower MBC for planktonic Gram-negative bacteria *P. aeruginosa* as compared with MBC of PS (>6 μM) proposed and investigated before (Meerovich et al. 2016; Tiganova et al. 2017).

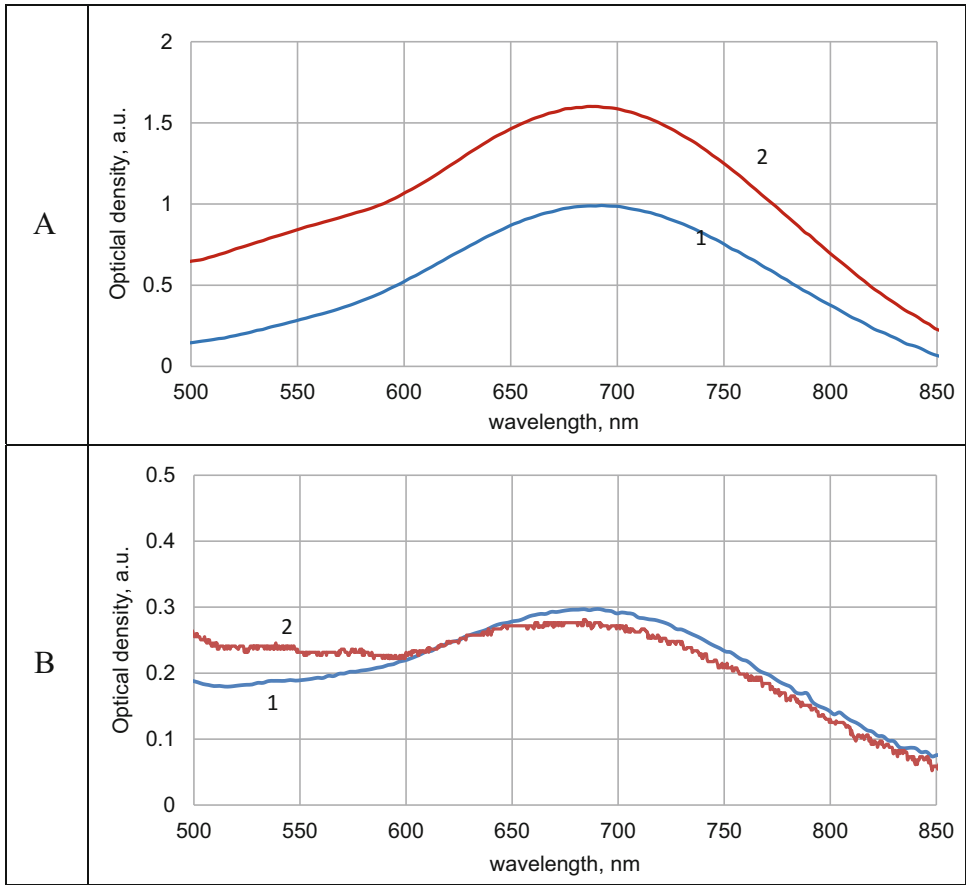

Fig. 9 The absorption spectra of pigments in the culture medium during biofilm growth of clinical isolates of *P. aeruginosa* 32 (**a**) and *P. aeruginosa* 21 (**b**): (1) by 24 h (by day 1) after the start of growth); (2) by 72 h (by day 3) after the start of growth

4.1 Photodynamic Inactivation of Bacterial Biofilms

Bacteria in biofilms are less susceptible to different influences, including PDI, so, higher concentrations of PS, a longer time of sensitization of biofilms and more light energy are need for their substantial inactivation.

The results of photodynamic inactivation of *P. aeruginosa 32* biofilms after 1 h incubation with the studied PS and irradiation with light dose of 100 J/cm^2 are shown in Fig. 11.

Inactivation of bacteria in biofilms depends on PS concentration during incubation and reached about 5 orders of magnitude with $(3\text{-PyEBr})_4\text{BCBr}_4$ and ZnPcChol_8. $(3\text{-PyEBr})_4\text{BCBr}_4$ had higher efficacy of photodynamic inactivation of *P. aeruginosa* biofilms compared with other studied photosensitizers. We suppose that smaller molecules of $(3\text{-PyEBr})_4\text{BCBr}_4$ have higher chance of penetration into the *P. aeruginosa* bacteria and more effectively diffuse through the matrix of the biofilm. Light loss for the excitation of this PS is less compared to ZnPcChol_8, since its excitation is carried out at 760 nm. These are the reasons for the high efficacy of $(3\text{-PyEBr})_4\text{BCBr}_4$.

The effectiveness of the *P. aeruginosa* bacteria inactivation in biofilms using ZnPcChol_8 was lower, since the molecules of ZnPcChol_8 have a molecular mass of 1678 Da and a lower probability of penetration into bacteria, and they are

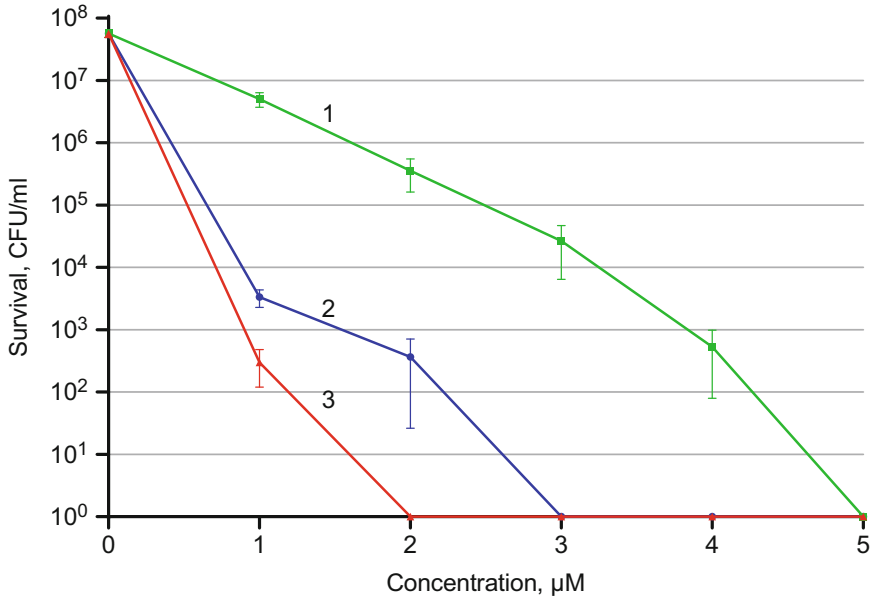

Fig. 10 Photoinactivation of planktonic bacteria *P. aeruginosa 32* depending of PS concentration: 1 – $ZnPcChol_8$; 2 – $(3\text{-}PyHp)_4BCBr_4$; 3 – $(3\text{-}PyEBr)_4BCBr_4$

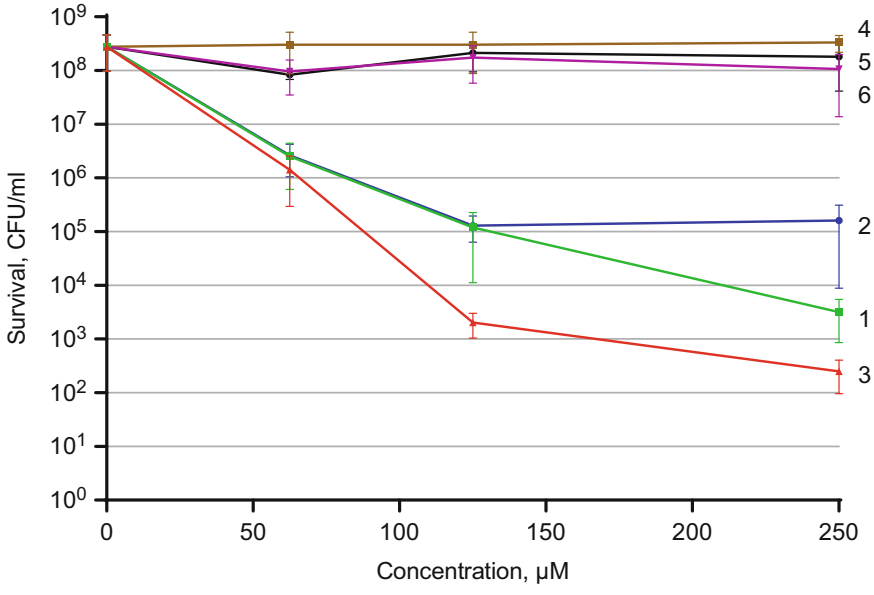

Fig. 11 Survival of *P. aeruginosa* in biofilms after PDI depending of PS concentration: 1, 2, 3 – after irradiation; 4, 5, 6-control without irradiation; 1, 4 – $ZnPcChol_8$; 2, 5 – $(3\text{-}PyHp)_4BCBr_4$; 3, 6 – $(3\text{-}PyEBr)_4BCBr_4$

excited in the spectral range of 680 nm, where the loss of exciting light due to the absorption of pigments in a biofilm is much higher.

The lower efficiency $(3\text{-}PyHp)_4BCBr_4$ in Kolliphor nanodispersion can be associated with a slower diffusion rate of Kolliphor nanoparticles through the matrix of biofilms.

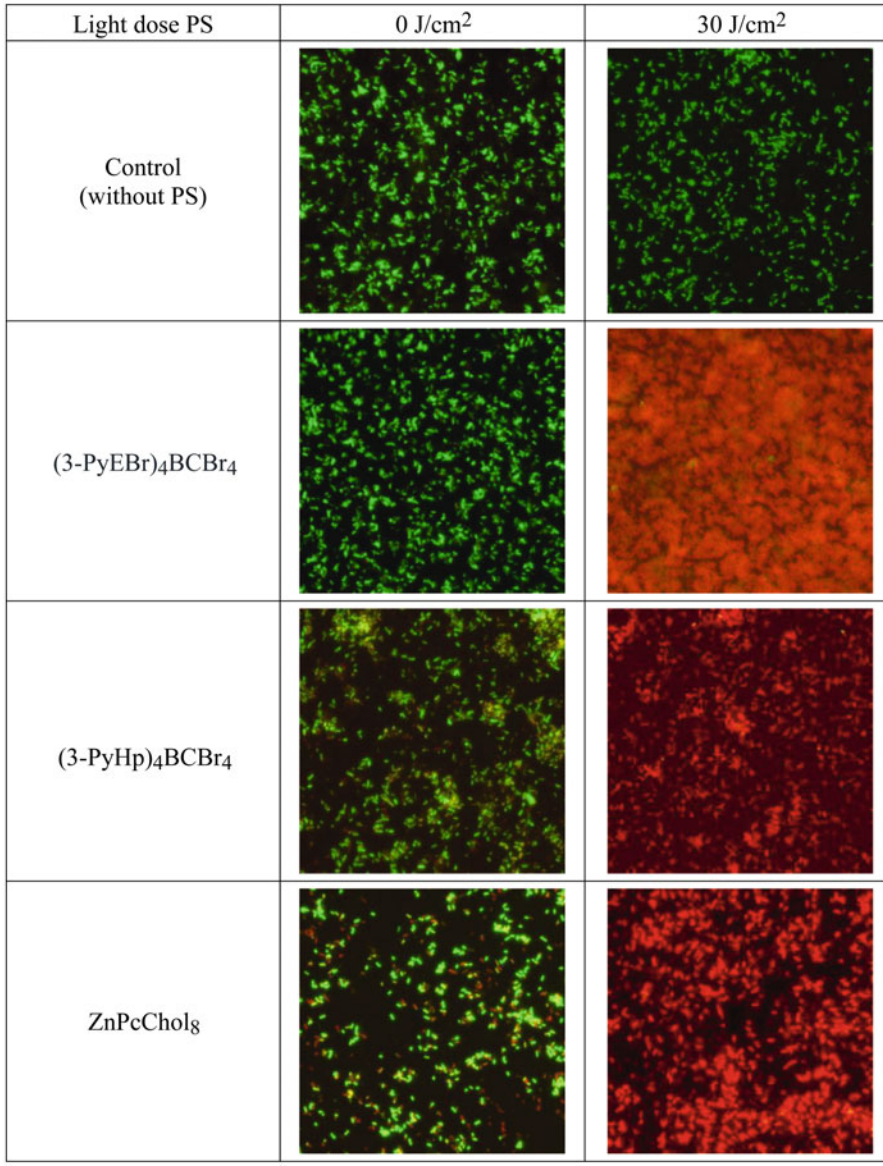

Fig. 12 The fluorescent microscopy images of *P. aeruginosa* biofilm before (left) and after (right) PDI using studied cationic PS

Fluorescent microscopy of biofilms after PDI and Live/Dead staining visualized the death of bacteria, or increasing of permeability of membranes, which is the first step of cell damage by reactive oxygen species after PDI. Damaged cells had red fluorescence due to staining with propidium iodide, which cannot enter the cells with intact membranes. We used a young biofilm because a mature one contains a large amount of extracellular DNA, which is also stained by propidium iodide and interferes visualization of bacteria. The results of fluorescent microscopy studies of *P. aeruginosa* 32 biofilms with studied PS and irradiation at 30 J/cm^2 are shown in Fig. 12. Live/Dead staining was not quantitative, but these pictures confirm that PDI using studied cationic PS provided effective inactivation of *P. aeruginosa* bacteria in biofilms.

5 Conclusion

Novel photosensitizers based on the derivatives of polyacationic phthalocyanines and synthetic bacteriochlorins have a high efficiency in photodynamic inactivation of Gram-negative bacteria *P. aeruginosa* as well as their biofilms *in vitro*. Tetracationic hydrophilic photosensitizer $(3\text{-PyEBr})_4\text{BCBr}_4$ with reduced molecular mass has higher efficacy of photodynamic inactivation of *P. aeruginosa* biofilms compared with other studied PS.

Studying the photophysical properties of PS in a wide range of concentrations demonstrated a low aggregation of these derivatives in water and serum. Consequently, their high photodynamic efficiency may be expected in in animal models enabling the use of these PS at high concentrations to sensitize pathological foci for APDT.

Some clinical isolates of *P. aeruginosa* produce pigments (in particular, pyocianine) in substantial amounts, which can significantly diminish light energy if excitation of PS occurs near 700 nm, thus protecting the bacteria from PDI. Photodynamic treatment using new bacteriochlorins with excitation at 760 nm, studied in this work, can overcome this difficulty; it facilitates the possibility of treating deep infected lesions *in vivo*.

References

Almeida A, Cunha A, Faustino MAF et al (2011) Porphyrins as antimicrobial photosensitizing agents. In: Hamblin MR, Jori G (eds) Photodynamic inactivation of microbial pathogens: medical and environmental applications. RSC Publishing, London, pp 83–160

Bertoloni G, Rossi F, Valduga G, Jori G et al (1992) Photosensitising activity of water- and lipid-soluble phthalocyanines on prokaryotic and eukaryotic microbial cells. Microbios 71(286):33–36

Bjarnsholt T, Jensen PO, Moser C, Hoiby N (2011) Biofilm infections. Springer, Heidelberg

Bystrov FG, Makarov VI, Pominova DV et al (2016) Analysis of photoluminescence decay kinetics of aluminum phthalocyanine nanoparticles interacting with immune cells. Biomed Photonics 5(1):3–8. https://doi.org/10.24931/2413-9432-2016-5-1-3-8

Cakir D, Gol C, Cakir V et al (2015) Water soluble {2-[3-(diethylamino)phenoxy]ethoxy} substituted zinc (II) phthalocyanine photosensitizers. J Lumin 159:79–87

Changenet-Barret P, Gustavsson T, Markovitsi D et al (2013) Unravelling molecular mechanisms in the fluorescence spectra of doxorubicin in aqueous solution by femtosecond fluorescence spectroscopy. Phys Chem Chem Phys 15(8):2937–2944

Chowdhary RK, Sharif I, Chansarkar N et al (2003) Correlation of photosensitizer delivery to lipoproteins and efficacy in tumor and arthritis mouse models; comparison of lipid-based and Pluronic P123 formulations. J Pharm Sci 6(2):198–204

Colak S, Durmus M, Yildiz SZ (2016) The water-soluble zwitterionic and cationic tetra-substituted zinc (II) phthalocyanines: synthesis, photophysical, photochemical and protein binding properties. Polyhedron 113:115–122

Dhami S, de Mello AJ, Rumbles G et al (1995) Phthalocyanine fluorescence at high concentration: dimers or reabsorption effect? Photochem Photobiol 61 (4):341–346. https://doi.org/10.1111/j.1751-1097.1995.tb08619.x

Di Palma MA, Alvarez MG, Durantini EN (2015) Photodynamic action mechanism mediated by zinc (II) 2,9,16,23-Tetrakis[4-(N-methylpyridyloxy)]-phthalocyanine in Candida Albicans cells. Photochem Photobiol 91(5):1203–1209

Dudkin SV, Efremenko AV, Ignatova AA et al (2013a) Photosensitizers for photodynamic therapy RU Patent 2476218, 2013

Dudkin SV, Ignatova AA, Kobzeva ES et al (2013b) Photosensitizer for photodynamic therapy. RU Patent 2479585, 2013

Dudkin SV, Makarova EA, Slivka LK et al (2014) Synthesis and properties of tetra- and octacationic meso-tetrakis(3-pyridyl)bacteriochlorin derivatives. J Porphyrins Phthalocyanines 18:107–114. https://doi.org/10.1142/s1088424613501162

El-Fouly MZ, Sharaf AM, Shahin AAM et al (2015) Biosynthesis of pyocyanin pigment by Pseudomonas aeruginosa. J Radiat Res Appl Sci 8(1):36–48. https://doi.org/10.1016/j.jrras.2014.10.007

Fonin AV, Sulatskaya AI, Kuznetsova IM et al (2014) Fluorescence of dyes in solutions with high absorbance. Inner filter effect correction. PLoS One 9(7):e103878. https://doi.org/10.1371/journal.pone.0103878

Griffith J, Shofield J, Wainwright M et al (1997) Some observations on the synthesis of polysubstituted zinc phthalocyanine sensitizers for photodynamic therapy. Dyes Pigments 33(1):65–78

Hamblin MR, Hasan T (2004) Photodynamic therapy: a new antimicrobial approach to infectious disease. Photochem Photobiol Sci 3(5):436–450

Huang L, Huang YY, Mroz P et al (2010) Stable synthetic cationic bacteriochlorins as selective antimicrobial photosensitizers. Antimicrob Agents Chemother 54:3834–3841

Juzenas P, Juzeniene A, Rotomskis R et al (2004) Spectroscopic evidence of monomeric aluminium phthalocyanine tetrasulphonate in aqueous solutions. J Photochem Photobiol B Biol 75(1–2):107–110. https://doi.org/10.1016/j.jphotobiol.2004.05.011

Ke M-R, Eastel J, Ngai K et al (2014) Photodynamic inactivation of bacteria and viruses using two monosubstituted zinc(II) phthalocyanines. Eur J Med Chem 84:278–283

Kuznetsova NA, Makarov DA, Yuzhakova OA et al (2006) Photosensitizing properties of polycationic Al and Zn phthalocyanines. J Porphyrins Phthalocyanines 10(4–6):627

Lourenço L, Sousa A, Gomes M et al (2015) Inverted methoxypyridinium phthalocyanines for PDI of pathogenic bacteria. Photochem Photobiol Sci 14 (10):1853–1863

Maisch T (2007) Anti-microbial photodynamic therapy: useful in the future? Lasers Med Sci 22(2):83. https://doi.org/10.1007/s10103-006-0409-7

Maisch T (2015) Resistance in antimicrobial photodynamic inactivation of bacteria. Photochem Photobiol 14(8):1518–1526. https://doi.org/10.1039/c5pp00037h

Makarov DA, Yuzhakova OA, Slivka LK et al (2007) Cationic Zn and Al phthalocyanines: synthesis, spectroscopy and photosensitizing properties. J Porphyrins Phthalocyanines 11(18):586–595

Makarov DA, Kuznetsova NA, Yuzhakova OA et al (2009) Effects of the degree of substitution on the physicochemical properties and photodynamic activity of zinc and aluminum phthalocyanine polycations. Russ J Phys Chem A 83:1044–1050

Makarova EA, Lukyanets EA, Tiganova IG et al (2018) Photosensitizers for photodynamic bacteria inactivation, including in biofilms. RU Patent 2670201, 2018

Mantareva VN, Angelov I, Wöhrle D et al (2013) Metallophthalocyanines for antimicrobial photodynamic therapy: an overview of our experience. J Porphyrins Phthalocyanines 17(6–7):399–416

Mass O, Lindsey JS (2011) A trans-AB-bacteriochlorin building block. J Org Chem 76(22):9478–9487. https://doi.org/10.1021/jo201967k

Meerovich GA, Tiganova IG, Makarova EA et al (2016) J Phy Conf Ser 691012011

Meerovich GA, Akhlyustina EV, Tiganova IG et al (2018) Photosensitizers for antibacterial photodynamic therapy based on tetracationic derivatives of synthetic bacteriochlorins. Laser Phys Lett 11:115602–115609. https://doi.org/10.1088/1612-202X/aae03f/

Minnock A, Vernon DI, Schofield J et al (1996) Photoinactivation of bacteria. Use of a cationic water-soluble zinc phthalocyanine to photoinactivate both gram-negative and gram-positive bacteria. J Photochem Photobiol B Biol 32:159–164

Moan J (1984) The photochemical yield of singlet oxygen from porphyrins in different states of aggregation. Photochem Photobiol 39:445–449. https://doi.org/10.1111/j.1751-1097.1984.tb03873.x

Nakonieczna J, Michta E, Rybicka M et al (2010) Superoxide dismutase is upregulated in Staphylococcus aureus following protoporphyrin-mediated photodynamic inactivation and does not directly influence the response to photodynamic treatment. BMC Microbiol 10:323. https://doi.org/10.1186/1471-2180-10-323

Nevonen DE, Makarova EA, King A, Lukyanets EA, Nemykin VN (2018) Elucidation of the electronic structure of water-soluble quaternized *meso*-Tetrakis (3-pyridyl)bacteriochlorin derivatives by experimental and theoretical methods. J Porphyrins Phthalocyanines 22(11):965–971

Newton H, Edwards J, Mitchell L, Percival SL (2017) Role of slough and biofilm in delaying healing in chronic wounds. Br J Nurs 26(Sup20a):S4–S11

Nikaido H (1994) Prevention of drug access to bacterial targets: permeability barrier and active efflux. Science 264(5157):382–388

Osifeko OL, Durmuş M, Nyokong T (2015) Physicochemical and photodynamic antimicrobial chemotherapy studies of mono- and tetra-pyridyloxy substituted indium(III) phthalocyanines. J Photochem Photobiol A Chem 301:47–54

Park YS, Lee HB, Chin S et al (2011) Acquisition of extensive drug-resistant Pseudomonas aeruginosa among hospitalized patients: risk factors and resistance mechanisms to carbapenems. J Hosp Infect 79 (1):54–58. https://doi.org/10.1016/j.jhin.2011.05.014

Percival SL, Suleman L, Francolini I, Donelli G (2014) The effectiveness of photodynamic therapy on planktonic cells and biofilms and its role in wound healing. Future Microbiol 9(9):1083–1094

Rocha D, Venkatramaiah N, Gomes M et al (2015) Photodynamic inactivation of *Escherichia coli* with cationic ammonium Zn(II) phthalocyanines. Photochem Photobiol Sci 14(10):1872–1879

Roncucci G, Dei D, Chiti G et al (2014) Antibacterial compositions comprising metal phthalocyanine analogues. US Patent No 8664382, 2014

Schastak S, Yafai Y, Geyer W et al (2008) Initiation of apoptosis by photodynamic therapy using a novel positively charged and water soluble near infra-red photosensitizer and white light irradiation. Methods Find Exp Clin Pharmacol 30:129–133

Schastak S, Ziganshyna S, Gitter B et al (2010) Efficient photodynamic therapy against gram-positive and gram-negative Bacteria using THPTS, a cationic photosensitizer excited by infrared wavelength. PLoS One 5(7): e11674. https://doi.org/10.1371/journal.pone.0011674

Segalla A, Borsarelli CD, Braslavsky SE et al (2002) Photophysical, photochemical and antibacterial photosensitizing properties of a novel octacationic Zn (II)-phthalocyanine. Antibacterial compositions comprising metal phthalocyanine analogues. Photochem Photobiol Sci 1(9):641–648

Simões C, Gomes M, Neves M et al (2016) Photodynamic inactivation of Escherichia coli with cationic meso-

tetraarylporphyrins. The charge number and charge distribution effects. Catal Today 266:197–204

Soncin M, Fabris C, Busetti A et al (2002) Approaches to selectivity in the Zn(II)-phthalocyanine-photosensitized inactivation of wild-type and antibiotic-resistant *Staphylococcus aureus*. Photochem Photobiol Sci 1(10):815–819

Spesia MB, Durantini EN (2013) Photodynamic inactivation mechanism of Streptococcus mitis sensitized by zinc(II) 2,9,16,23-tetrakis[2-(N,N,N-trimethylamino) ethoxy]phthalocyanine. J Photochem Photobiol B Biol 125:179–187

Strakhovskaya MG, Antonenko YN, Pashkovskaya AA et al (2009) Electrostatic binding of substituted metallophthalocyanines with enterobacteria cells: role of photodynamic inactivation. Biokhimiya/Biochemistry 74(12):1603–1614

Tavares A, Carvalho CMB, Faustino MA et al (2010) Antimicrobial photodynamic therapy: study of bacterial recovery viability and potential development of resistance after treatment. Mar Drugs 8(1):91–105. https://doi.org/10.3390/md8010091

Tiganova IG, Makarova EA, Meerovich GA et al (2017) Photodynamic inactivation of pathogenic bacteria in biofilms using new synthetic bacterioclorin derivatives. Biomed Photonics 6(4):27–36

Tominaga TT, Yusbmanov VE, Borissevitchl E et al (1997) Aggregation phenomena in the complexes of iron tetraphenylporphinesulfonate with bovine serum albumin. J Inorg Biochem 65:235–244

Usacheva MN, Teichert MC, Biel MA (2001) Comparison of the methylene blue and toluidine blue photobactericidal efficacy against gram-positive and gram-negative microorganisms. Lasers Surg Med 29:165–173

van Lier JE, Spikes JD (1989) The chemistry, photophysics and photosensitizing properties of phthalocyanines. In: Photosensitizing compounds: their chemistry, biology and clinical use, Ciba foundation symposium, 1989, 146:17–32, Wiley, Chichester

Vecchio D, Dai T, Huang L et al (2013) Antimicrobial photodynamic therapy with RLP068 kills methicillin-resistant *Staphylococcus aureus* and improves wound healing in a mouse model of infected skin abrasion. J Biophotonics 6(9):733–742

Vera DM, Haynes MH, Ball AR et al (2012) Strategies to potentiate antimicrobial photoinactivation by overcoming resistant phenotypes. Photochem Photobiol 88(3):499–511. https://doi.org/10.1111/j.1751-1097.2012.01087.x

Vorozhtsov GN. Kaliya OL, Kuznetsova NA et al (2006a) Photosensitizers for antimicrobial photodynamic therapy. RU Patent 2282647 (27.08.2006)

Vorozhtsov GN, Karmakova TA, Luzhkov YuM et al (2006b) Photosensitizers for photodynamic therapy. RU Patent 2282646 (27.08.2006)

Yakubovskaya RI, Morozova NB, Pankratov AA et al (2015) Experimental photodynamic therapy: 15 years of development. Russ J Gen Chem 85(1):217–239

Yuzhakova OA, Negrimovsky VM, Kuznetsova NA et al (2005) Method of preparation of zinc phthalocyanine. RU Patent 2281952 (2005)

Yuzhakova OA, Kuznetsova NA, Lukyanets EA et al (2010) Method of phthalocyanines chloromethylation. RU Patent 2405785 (2010)

Zhang L, Wang A, Lu S et al (2015) The influences of the number of the ammonium groups and their arrangement manner on the photophysical properties of the quaternized zinc phthalocyanines. Inorg Chem Commun 53:15–19

Zheng B-Y, Zhang H-P, Ke M-R, Huang J-D (2013) Synthesis and antifungal photodynamic activities of a series of novel zinc(II) phthalocyanines substituted with piperazinyl moieties. Dyes Pigments 99 (1):185–191